

# From Noise Estimation to Restoration: A Unified Diffusion and Bayesian Risk Approach for Unsupervised Denoising

Reeshad Khan<sup>a</sup>, Ukash Nakarmi<sup>b</sup> and John M. Gauch<sup>c</sup>

*Department of Electrical Engineering and Computer Science, University of Arkansas, Fayetteville, Arkansas, U.S.A.  
{rk010, unakarmi, jgauch}@uark.edu*

**Keywords:** Diffusion, Stein’s Unbiased Risk Estimator, Bayesian Loss, SURE, PURE, PGURE, MRI Denoising, Unsupervised Learning.

**Abstract:** Deep Neural Networks (DNNs) have revolutionized image denoising, challenging traditional methods such as Stein’s Unbiased Risk Estimator (SURE) and its extensions (eSURE and PURE), along with Extended Poisson Unbiased Risk Estimator (ePURE). These traditional approaches often struggle to generalize across different noise types, especially when noise characteristics are unknown or vary widely, and they are not equipped to handle mixed noise scenarios effectively. In response, we present a novel unsupervised learning strategy that leverages an enhanced diffusion model combined with a dynamically trained Deep Convolutional Neural Network (DnCNN). We introduce adaptive Bayesian loss functions—Bayesian-SURE, Bayesian-PURE, and a newly developed Bayesian-Poisson-Gaussian Unbiased Risk Estimator (Bayesian-PGURE)—that adjust to estimated noise levels and types without prior knowledge. This innovative method enables significant improvements in handling mixed noise conditions and ensures robustness across varied imaging scenarios. Our comprehensive evaluations on MRI data corrupted by Gaussian, Poisson, and mixed noise demonstrate that our approach outperforms existing algorithms, achieving superior denoising performance and image fidelity under diverse, unpredictable conditions. Our contributions advance the state-of-the-art in medical imaging denoising, establishing a new benchmark for unsupervised learning frameworks in managing complex noise dynamics.


## 1 INTRODUCTION


Magnetic Resonance Imaging (MRI) serves as a critical tool in clinical diagnostics due to its non-ionizing nature and superior tissue contrast capabilities, offering safe imaging without radiation exposure (Jalata et al., 2024). Despite these advantages, MRI scans are inherently affected by noise introduced during the acquisition process, which often necessitates advanced denoising techniques to improve image quality (Manjón and Coupe, 2019). While traditional denoising methods like BM3D (Burger et al., 2012) have been effective for synthetic noise types such as Gaussian (Zhang et al., 2017a) and Poisson (Cherry et al., 2012), the advent of Deep Learning (DL) has shifted paradigms towards more adaptive, data-driven approaches.


Deep Neural Networks (DNNs) have demonstrated a remarkable ability to manage both synthetic

and realistic noise scenarios, outperforming classical methods under diverse conditions. However, the conventional training of DNN-based denoisers often relies on the availability of pristine, noiseless ground truth images—a requirement seldom met in practical scenarios (Zhussip et al., 2019). This challenge has led to the development of unsupervised learning techniques such as Deep Image Prior (DIP) (Ulyanov et al., 2020) and Noise2Noise (Lehtinen et al., 2018a), which leverage the inherent capabilities of DNNs to reconstruct high-quality images from noisy data without needing clean examples (Ulyanov et al., 2018), (Lehtinen et al., 2018b).

Building upon the foundations of Stein’s Unbiased Risk Estimator (SURE) (Metzler et al., 2020) and its variants eSURE (Zhussip et al., 2019), Poisson Unbiased Risk Estimator (PURE) (Kim et al., 2022), and Extended Poisson Unbiased Risk Estimator (ePURE) (Kim et al., 2022), our work introduces an innovative unsupervised framework that combines an enhanced diffusion model (Ho et al., 2020) with a dynamically trained DnCNN (Zhang et al., 2017b). This approach

<sup>a</sup>  <https://orcid.org/0009-0008-9870-022X>

<sup>b</sup>  <https://orcid.org/0000-0002-5351-3956>

<sup>c</sup>  <https://orcid.org/0009-0008-7417-1212>

not only addresses the limitations of existing methods—particularly their struggles with generalization across unknown or mixed noise types—but also sets new benchmarks in MRI denoising.

Our method leverages Bayesian-enhanced loss functions—Bayesian-SURE, Bayesian-PURE, and Bayesian-Poisson-Gaussian Unbiased Risk Estimator (Bayesian-PGURE)—which dynamically adapt to the estimated noise characteristics, thus allowing for robust denoising performance even when the noise type and level are not a priori known. This adaptive capability is crucial for practical applications where noise properties can significantly vary, such as in medical imaging environments (Kim et al., 2020), (Kim et al., 2022).

Furthermore, we extend the theoretical understanding of unsupervised denoising by drawing connections between our Bayesian-enhanced methods and the Noise2Noise framework, suggesting that our Bayesian approaches can be viewed as a generalization capable of handling correlated noise scenarios more effectively (Lehtinen et al., 2018b). The experimental validation of our models on MRI datasets contaminated with Gaussian, Poisson, and mixed noise types demonstrates superior performance over traditional methods, particularly in scenarios where the noise characteristics deviate from standard assumptions.

Our contributions not only advance the state-of-the-art in image denoising but also open avenues for future research into unsupervised learning models that can seamlessly adapt to varied and dynamically changing environmental conditions, thereby significantly impacting both the theory and application of machine learning in medical imaging.

## 2 BACKGROUND

The evolution of image denoising techniques, particularly for medical applications such as MRI, has required a deep understanding of both traditional and advanced methodologies. This section introduces the foundational concepts and established estimators, setting the stage for the innovative approaches we develop in subsequent sections. The core of our approach leverages Stein’s Unbiased Risk Estimator (SURE) and its Monte Carlo variant (MC-SURE), frameworks that have been extensively validated in other domains. Our work extends the application of these established methods to the complex noise characteristics inherent in MRI data, a domain where the acquisition of noise-free ground truth is notably challenging.

We review the principles of SURE (Metzler et al., 2020) and MC-SURE, discussing their theoretical underpinnings and the rationale behind their effectiveness in scenarios lacking clean data. By adapting these methods to the realm of medical imaging, specifically to MRI, we aim to demonstrate their robustness and utility in a field where accurate image restoration is critical yet burdened by inherent noise. This adaptation not only underscores the versatility of these estimators across various applications but also sets the stage for detailed examinations of their performance in the subsequent sections of this study.

### 2.1 Stein’s Unbiased Risk Estimator (SURE)

In the context of denoising Gaussian-contaminated signals or images, a typical model involves a linear equation:

$$y = x + n \quad (1)$$

where  $x \in \mathbb{R}^N$  represents an unknown signal,  $y \in \mathbb{R}^N$  is the observed noisy measurement, and  $n \in \mathbb{R}^N$  denotes i.i.d. Gaussian noise with  $n \sim \mathcal{N}(0, \sigma^2 I)$ , where  $I$  is the identity matrix.

The SURE (Stein’s Unbiased Risk Estimator) (Metzler et al., 2020) is a widely-used approach to estimate the mean squared error (MSE) associated with an estimator  $h(y)$  of  $x$ . It is given by the expression:

$$\eta(h(y)) = \frac{\|y - h(y)\|^2}{N} - \sigma^2 + \frac{2\sigma^2}{N} \sum_{i=1}^N \frac{\delta h_i(y)}{\delta y_i} \quad (2)$$

This equation suggests that the random variable  $\eta(h(y))$  is an unbiased estimator of the MSE of  $h(y)$ , given by:

$$\mathbb{E}_{n \sim \mathcal{N}(0, \sigma^2)} \left\{ \frac{\|x - h(y)\|^2}{N} \right\} = \mathbb{E}_{n \sim \mathcal{N}(0, \sigma^2)} \{ \eta(h(y)) \} \quad (3)$$

Obtaining an analytical solution for the divergence term in equation (2) is limited to special cases, such as when the estimator  $h(y)$  is a non-local mean or linear filter. To utilize (2) in more general cases, an approximate solution for the divergence term is necessary.

### 2.2 Poisson Unbiased Risk Estimator (PURE)

The Poisson Unbiased Risk Estimator (PURE) (Kim et al., 2022) is designed to address denoising scenarios where the noise model is strictly Poissonian, often relevant in medical imaging and photon-limited imaging environments. The model for PURE (Kim et al., 2022) is expressed by:

$$y = x + n_p \quad (4)$$

where  $x \in \mathbb{R}^N$  denotes the true signal,  $y \in \mathbb{R}^N$  is the observed image, and  $n_p \in \mathbb{R}^N$  represents Poisson noise, which is signal-dependent, differing from Gaussian noise.

The PURE (Kim et al., 2022) estimator for the mean squared error (MSE) of an estimator  $h(y)$  of  $x$ , considering Poisson noise, is given by:

$$\eta_{PURE}(h(y)) = \sum_{i=1}^N (h_i(y) - y_i \log(h_i(y))) \quad (5)$$

This estimator effectively leverages the log-likelihood of Poisson-distributed data, providing a robust framework for noise estimation and image restoration under Poisson noise conditions.

### 2.3 Poisson Unbiased Risk Estimator (PURE) and Poisson-Gaussian Unbiased Risk Estimator (PGURE)

Following the Gaussian noise scenario and inspired by (Luisier et al., 2011), we extend our approach to address mixed noise conditions commonly encountered in medical imaging and other photon-limited imaging applications. PURE (Kim et al., 2022) and PGURE provide frameworks to handle purely Poisson noise and a combination of Poisson and Gaussian noise, respectively.

PGURE, in particular, is described by the following loss function, adapted for noise levels that are not known beforehand and may vary spatially or temporally across the image:

$$\eta_{PGURE}(h(y)) = \sum_{i=1}^N (h_i(y) - y_i \log(h_i(y))) - \hat{\sigma}^2 + \frac{2\hat{\sigma}^2}{N} \sum_{i=1}^N \frac{\delta h_i(y)}{\delta y_i} \quad (6)$$

This formulation incorporates the Bayesian approach to dynamically estimate both the parameters of Poisson ( $\lambda$ ) and Gaussian ( $\sigma^2$ ) noise components, allowing for a more precise and adaptable denoising process.

### 2.4 Monte-Carlo SURE (MC-SURE)

MC-SURE is a Monte Carlo method proposed by Ramani et al. (Ramani et al., 2008) to estimate the divergence and, consequently, the SURE loss.

Assume  $\tilde{b} \sim \mathcal{N}_{0,1} \in \mathbb{R}^N$  is a Gaussian vector which is independent of  $n$  or  $y$ . Ramani et al (Ramani et al., 2008) show that,

$$\sum_{i=1}^K \frac{\delta h_i(y)}{\delta y_i} = \lim_{\varepsilon \rightarrow 0} \mathbb{E}_{\tilde{b}} \left\{ \tilde{b}^T \left( \frac{h(y + \varepsilon \tilde{b}) - h(y)}{\varepsilon} \right) \right\} \quad (7)$$

Therefore, by applying this eq 7 to the divergence term in eq 2:

$$\frac{1}{N} \sum_{i=1}^N \frac{\delta h_i(y)}{\delta y_i} \approx \frac{1}{\varepsilon N} \tilde{b}^T (h(y + \varepsilon \tilde{b}) - h(y)) \quad (8)$$

Here,  $\tilde{b}^T$  is the transpose of  $\tilde{b}$ , and  $\varepsilon$  is a small positive value to approximate the limit.

## 3 METHODS

This section outlines our innovative approach for unsupervised image denoising, leveraging a diffusion-based model (Ho et al., 2020) for dynamic noise estimation combined with Bayesian formulations of SURE, PURE, and PGURE for training our denoiser. Our method significantly enhances the adaptability and effectiveness of deep learning denoisers in handling various real-world noise types without the need for paired clean and noisy images.

### 3.1 Noise Estimation Using Diffusion Models

Our approach utilizes a diffusion model (Ho et al., 2020) as a dynamic noise estimator, which is trained to predict both the type and level of noise directly from noisy images. This model operates by gradually adding noise to a clean image and learning to reverse this process, thereby predicting the noise characteristics at each step.

For Gaussian noise, the model adds and reverses noise as follows:

$$\text{Diffusion: } x_{t+1} = \sqrt{1 - \beta_t} x_t + \sqrt{\beta_t} \varepsilon, \quad \varepsilon \sim \mathcal{N}(0, I), \quad (9)$$

$$\text{Reverse: } x_{t-1} = \frac{x_t - \sqrt{\beta_t} \varepsilon_\theta(x_t, t)}{\sqrt{1 - \beta_t}}, \quad (10)$$

For Poisson noise, the diffusion equations adapt to the signal-dependent nature:

$$\text{Diffusion: } x_{t+1} = \sqrt{1 - \beta_t} x_t + \sqrt{\beta_t} \varepsilon_p, \quad \varepsilon_p \sim \text{Poisson}(\lambda), \quad (11)$$

$$\text{Reverse: } x_{t-1} = \frac{x_t - \sqrt{\beta_t} \lambda_\theta(x_t, t)}{\sqrt{1 - \beta_t}} \quad (12)$$

where  $\beta_t$  are the variance schedules,  $\varepsilon$  and  $\varepsilon_p$  represent Gaussian and Poisson noise, respectively, and  $\varepsilon_\theta, \lambda_\theta$  are the noise levels predicted by the model.

### Noise Type and Level Prediction

Within the framework of the diffusion model (Ho et al., 2020), the noise type (e.g., Gaussian, Poisson) and its corresponding level (parameters such as  $\sigma$  for Gaussian or  $\lambda$  for Poisson) are predicted by an auxiliary neural network module:

$$\hat{\sigma}, \hat{\lambda} = f_{\theta}(x_t, t) \quad (13)$$

where  $f_{\theta}$  represents the neural network trained to predict noise parameters based on the diffused image  $x_t$  and timestep  $t$ . This prediction enables tailoring the denoising process to the specific characteristics of the noise, enhancing the effectiveness of subsequent denoising steps.

### 3.2 Bayesian SURE, PURE, and PGURE

Utilizing the estimated noise parameters, we compute the Bayesian versions of the SURE, PURE, and PGURE losses for training our denoising network. These losses adapt to the estimated noise levels and types, providing a flexible framework for training under varying noise conditions.

#### Custom Bayesian Loss Formulations

To address the variations in noise type and intensity, we introduce custom Bayesian loss functions that dynamically adjust based on the estimated noise characteristics:

Bayesian SURE (BSURE) is designed for Gaussian noise environments and is formulated as:

$$L_{\text{BSURE}} = \text{MSE}(y, \hat{y}) - \sigma^2 + 2\sigma^2 \cdot \text{div}(\hat{y}, y)$$

where MSE is the mean squared error,  $\sigma$  is the estimated noise level,  $\hat{y}$  is the denoised image,  $y$  is the noisy image, and  $\text{div}$  represents the divergence estimated via a Monte Carlo approach.

Bayesian PURE (BPURE) applies to Poisson noise conditions:

$$L_{\text{BPURE}} = \hat{y} - y \log(\hat{y}) + \lambda - y \log(\lambda)$$

where  $\lambda$  is the estimated Poisson noise level.

Bayesian PGURE (BPGURE) is used for mixed noise scenarios, combining the features of BSURE and BPURE.

These loss functions are weighted dynamically based on the predicted noise type, ensuring optimal denoising performance across different imaging conditions. This approach not only enhances the generalizability of the model but also tailors the denoising process to effectively handle the specific noise characteristics present in medical imaging, where noise types can vary significantly.

### 3.3 Modified Bayesian SURE (Bayesian-SURE)

Our research introduces a Bayesian adaptation of the SURE (Metzler et al., 2020) framework, termed Bayesian-SURE, which incorporates a prior distribution on the noise level, allowing for a dynamic estimation process that is more robust in practical settings where the noise level might not be known a priori. This approach utilizes a Bayesian inference method to estimate the noise variance  $\sigma^2$  dynamically:

$$\eta_{\text{Bayesian-SURE}}(h(y)) = \frac{\|y - h(y)\|^2}{N} - \hat{\sigma}^2 + \frac{2\hat{\sigma}^2}{N} \sum_{i=1}^N \frac{\delta h_i(y)}{\delta y_i} \quad (14)$$

Here,  $\hat{\sigma}^2$  represents the estimated noise variance derived from the Bayesian posterior, enhancing the flexibility and adaptability of the SURE method to varying noise conditions.

### 3.4 Enhanced Monte-Carlo SURE (MC-SURE)

In our project, we propose a modified Monte Carlo SURE estimator to enhance the accuracy and reduce the variance of the divergence estimation, crucial for effective denoising performance. The traditional MC-SURE, as described by Ramani et al. (Ramani et al., 2008), relies on a single Gaussian perturbation vector  $\tilde{b}$  to estimate the divergence term crucial for the SURE loss calculation.

Our enhancement involves averaging multiple independent estimations of the gradient, each derived from a distinct Gaussian vector. This modification is inspired by the Central Limit Theorem, which suggests that averaging a set of independent estimates reduces variance, leading to a more robust and stable estimator. The modified equation is as follows:

$$\frac{1}{N} \sum_{i=1}^N \frac{\delta h_i(y)}{\delta y_i} \approx \frac{1}{M\epsilon N} \sum_{j=1}^M \tilde{b}_j^T (h(y + \epsilon \tilde{b}_j) - h(y)) \quad (15)$$

where  $M$  is the number of independent Gaussian vectors  $\tilde{b}_j$ , each sampled anew for the estimation. This approach mitigates the noise in the gradient estimation by averaging over multiple perturbations, thus leading to a more accurate and reliable estimate of the divergence.

This modification not only enhances the reliability of the SURE loss estimate but also stabilizes the optimization process in iterative denoising methods, potentially resulting in higher quality reconstructions

and improved generalization across different noise conditions.

### 3.5 Modified Bayesian PURE (Bayesian-PURE)

To enhance the PURE framework, we introduce a Bayesian adaptation, termed Bayesian-PURE, which incorporates Bayesian principles to dynamically estimate the parameters of the Poisson distribution, particularly the rate parameter  $\lambda$ . This modification allows for adapting to varying noise levels across different image regions, enhancing the estimator’s flexibility and accuracy in practical imaging scenarios.

The Bayesian-PURE is formulated as follows:

$$\eta_{\text{Bayesian-PURE}}(h(y)) = \sum_{i=1}^N (h_i(y) - y_i \log(h_i(y))) + \frac{1}{N} \sum_{i=1}^N (\lambda_i - y_i \log(\lambda_i)) \quad (16)$$

Here,  $\lambda_i$  represents the estimated Poisson rate for each pixel, derived from a Bayesian posterior that accounts for the observed data. This approach not only improves the adaptability of the estimator to different noise conditions but also enhances the accuracy of denoising in environments where noise characteristics may not be uniform or are unknown a priori.

### 3.6 Optimization of Deep Denoisers via Enhanced SURE-Derived Losses

The integration of Stein’s Unbiased Risk Estimator (SURE) and its variants, including Poisson Unbiased Risk Estimator (PURE) and Poisson-Gaussian Unbiased Risk Estimator (PGURE), has significantly advanced the unsupervised optimization of deep neural network (DNN)-based denoisers. Our work extends these methodologies by incorporating Bayesian principles, which dynamically adjust to the noise characteristics estimated from the data, thereby eliminating the need for pristine ground truth images—a common limitation in supervised learning paradigms.

We have developed modified Bayesian SURE, PURE, and PGURE frameworks, which employ a Bayesian approach to dynamically estimate noise parameters and apply these estimations to optimize the training process of DNNs. These modifications allow for adaptive loss functions that are tailored to the estimated type and level of noise, enhancing the flexibility and effectiveness of the denoising process. The Bayesian-enhanced loss functions are defined as follows:

$$\eta_{\text{Bayesian}}(h_{\theta}(\mathbf{y})) = \frac{1}{M} \sum_{j=1}^M \left\{ \|\mathbf{y}^{(j)} - h_{\theta}(\mathbf{y}^{(j)})\|^2 - \hat{\sigma}_j^2 + \frac{2\hat{\sigma}_j^2}{\epsilon} (\tilde{\mathbf{b}}^{(j)})^T (h_{\theta}(\mathbf{y}^{(j)} + \epsilon \tilde{\mathbf{b}}^{(j)}) - h_{\theta}(\mathbf{y}^{(j)})) \right\}. \quad (17)$$

where  $M$  denotes the batch size,  $\mathbf{y}^{(j)}$  represents the  $j$ -th noisy image in the batch,  $\hat{\sigma}_j^2$  is the dynamically estimated noise variance for the  $j$ -th image, and  $\tilde{\mathbf{b}}^{(j)}$  is an auxiliary Gaussian perturbation vector independent of the noise inherent in  $\mathbf{y}$ . This reformulation not only accounts for the direct error and the noise variance adjustment but also incorporates a Monte Carlo estimation of the divergence term, providing a robust and adaptive framework for the MSE, which is typically inaccessible in unsupervised settings.

Our experiments demonstrate that this approach not only streamlines the training process by removing the necessity for clean data but also significantly enhances the neural network’s ability to generalize from noisy inputs. By effectively learning to denoise through a self-supervised learning framework, our models achieve superior performance across various noise conditions, demonstrating robustness and adaptability in real-world denoising tasks.

## 4 EXPERIMENTS AND RESULTS

In this section, we evaluate our proposed Bayesian-enhanced diffusion model (Ho et al., 2020) and DnCNN (Zhang et al., 2017b) framework on a challenging MRI dataset and compare its performance to existing denoising methods. We first describe the dataset and preprocessing steps, followed by preliminary experiments with traditional methods. We then present the results of our Bayesian approach under various noise conditions and provide a detailed analysis of its performance.

### 4.1 Dataset and Preprocessing

We use fully-sampled 3T knee MRI scans from 22 subjects (11 males and 11 females) as described in (Anonymous, 2013). Each subject’s volume is segmented into  $320 \times 320 \times 256$  matrices and sliced into  $320 \times 256$  axial planes. MRI acquisition was performed using a 3T whole-body scanner, and raw k-space data were preserved for authenticity.

From these volumes, we generated both axial and coronal view PNG images for training and evaluation. We used 1000 axial and 1000 coronal images for training, with 100 images per view for testing. This

setup ensures a diverse set of anatomical variations and noise conditions.

## 4.2 Preliminary Experiments with Traditional Methods

Before evaluating our Bayesian approach, we conducted preliminary experiments using methods such as SURE (Metzler et al., 2020), eSURE (Zhussip et al., 2019), PURE (Kim et al., 2022), ePURE (Kim et al., 2022), Noise2Noise (N2N) (Lehtinen et al., 2018a), BM3D (Dabov et al., 2007), and DnCNN (Zhang et al., 2017b) trained with standard MSE and known ground truth. We tested these methods on controlled Gaussian noise levels ( $\sigma = 25$  and  $\sigma = 50$ ) for both axial and coronal views.

The Peak Signal-to-Noise Ratio (PSNR) results are presented in Table 1. As shown, eSURE (Zhussip et al., 2019) and N2N methods perform strongly under known Gaussian conditions, achieving high PSNR values.

These preliminary results highlight the strengths and limitations of traditional methods. While some methods excel under known, controlled conditions, they are not as robust when noise characteristics differ from assumptions.

## 4.3 Bayesian-Enhanced Diffusion Model Evaluation

We now evaluate our Bayesian-enhanced diffusion model integrated with DnCNN (Zhang et al., 2017b) under various unknown noise conditions (Gaussian, Poisson, and mixed). Unlike the preliminary experiments, our approach does not assume prior knowledge of noise parameters.

Table 2 summarizes PSNR and SSIM results under unknown Gaussian and Poisson noise levels, as well as a mixed scenario. Our Bayesian approach achieves notably higher PSNR and SSIM compared to baseline methods, demonstrating its adaptability.

To visually illustrate these improvements, Figure 1 shows denoised axial views under Gaussian noise. The Bayesian-enhanced model restores fine details and texture more faithfully than baseline methods.

Figure 2 highlights denoising performance on coronal views. Again, our approach demonstrates robustness and edge fidelity, even under higher noise levels.

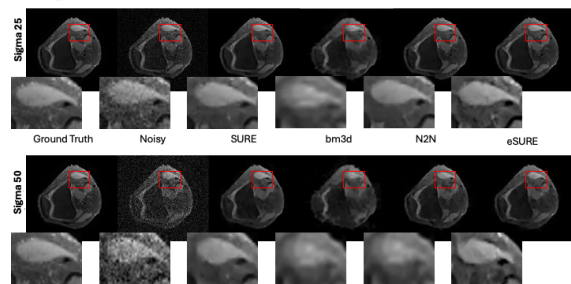


Figure 1: Denoised results for axial views under Gaussian noise ( $\sigma = 25$  and  $50$ ). Our Bayesian model preserves details and edges more effectively.

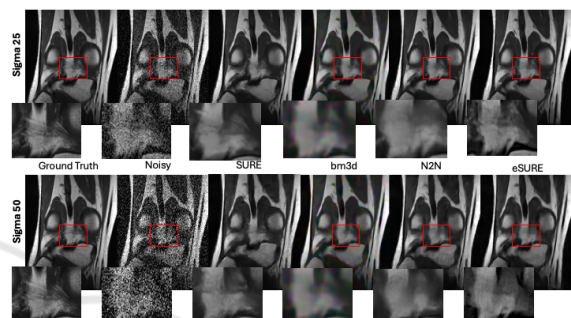


Figure 2: Denoised results for coronal views under Gaussian noise ( $\sigma = 25$  and  $50$ ). The proposed method maintains structural details better than competitors.

## 4.4 Visualizing Results on Poisson and Mixed Noise

To further assess performance in complex scenarios, we tested on Poisson and mixed noise. Figure 3 provides a comparison under Poisson noise at different intensities using ePURE, and Figure 4 shows results under Gaussian, Poisson, and mixed noise types without prior knowledge of noise parameters. Our model adapts seamlessly, producing high-quality reconstructions across all conditions.

## 4.5 Mixed Noise Scenarios and Gradual Intensity Changes

In practical MRI settings, noise profiles may vary across scans or within a single volume. Figure 5 illustrates our model's performance on mixed noise with gradually increasing intensity (from  $\sigma = 10$  to  $50$  and  $\lambda = 0.2$  to  $1.0$ ). Even as noise intensity changes, the Bayesian-enhanced approach retains stable performance and reconstructs subtle structures that other methods fail to recover.

Finally, Table 3 presents PSNR and SSIM results under Poisson noise for ePURE, further validating the competitiveness and adaptability of our approach.

Table 1: PSNR results of blind denoisers in preliminary experiments on 3T Knee MRI. Higher is better.

3T Knee MRI Axial View						
Methods	BM3D	DnCNN-SURE	DnCNN-SURE*	DnCNN-N2N	DnCNN-eSURE	DnCNN-MSE
$\sigma = 25$	29.10	31.56	29.00	<b>33.96</b>	<b>33.96</b>	29.20
$\sigma = 50$	27.75	31.55	26.07	31.53	<b>31.63</b>	26.22
3T Knee MRI Coronal View						
Methods	BM3D	DnCNN-SURE	DnCNN-SURE*	DnCNN-N2N	DnCNN-eSURE	DnCNN-MSE
$\sigma = 25$	29.10	32.55	29.00	32.46	<b>32.56</b>	30.82
$\sigma = 50$	27.75	28.75	26.07	28.86	<b>29.99</b>	28.83

Table 2: PSNR and SSIM results of the Bayesian-enhanced diffusion model on MRI data. The method adapts to unknown and mixed noise scenarios.

Metrics	$\sigma = 25$	$\sigma = 50$	$\lambda = 0.5$	$\lambda = 1.0$
PSNR	35.05	32.80	33.25	30.00
SSIM	0.95	0.92	0.94	0.90

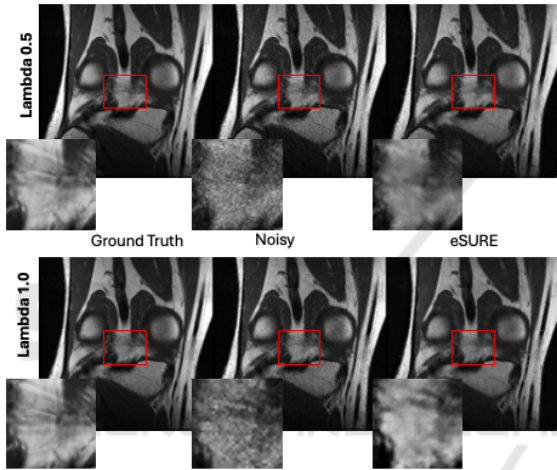


Figure 3: Visual comparison under Poisson noise at varying intensities using ePURE. Our Bayesian approach adapts to different noise levels, enhancing image fidelity.

Table 3: PSNR and SSIM results for ePURE on 3T Knee MRI Coronal View under Poisson noise.

Noise Level	PSNR	SSIM
$\lambda = 0.5$	31.68	0.934
$\lambda = 1.0$	32.45	0.947

### 4.6 Discussion of Results

Our experiments demonstrate that the Bayesian-enhanced diffusion framework outperforms traditional methods that rely on known noise models. By dynamically estimating noise characteristics, the model adapts to diverse conditions without ground truth. The result is a more flexible, generalizable denoising tool suitable for real-world MRI scenarios.

The visual and quantitative evidence suggests that this approach maintains structural integrity and detail fidelity in conditions that break assumptions made by

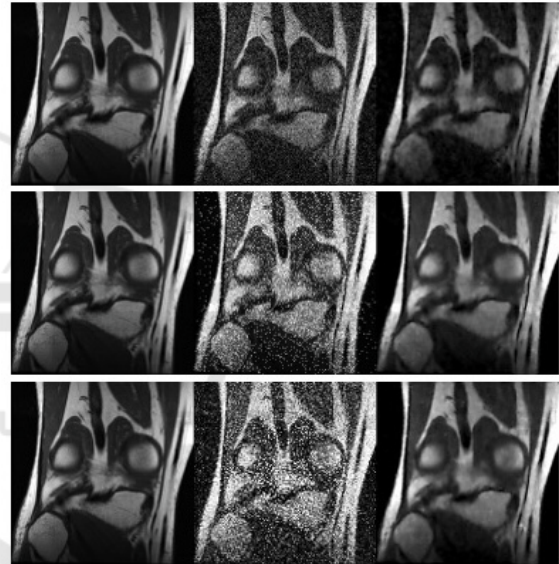


Figure 4: Denoised results for Gaussian, Poisson, and mixed noise (top to bottom) with unknown parameters. Our method generalizes well, delivering consistent quality.

classical methods. Consequently, it sets a new standard for unsupervised denoising under complex, variable noise patterns.

## 5 CONCLUSION

This work presents a novel unsupervised learning framework for MRI denoising that integrates an enhanced diffusion model with a dynamically trained Deep Convolutional Neural Network (DnCNN) (Zhang et al., 2017b). By employing adaptive loss functions that adjust to dynamically estimated noise characteristics, our approach facilitates robust denoising across a wide range of conditions without requir-

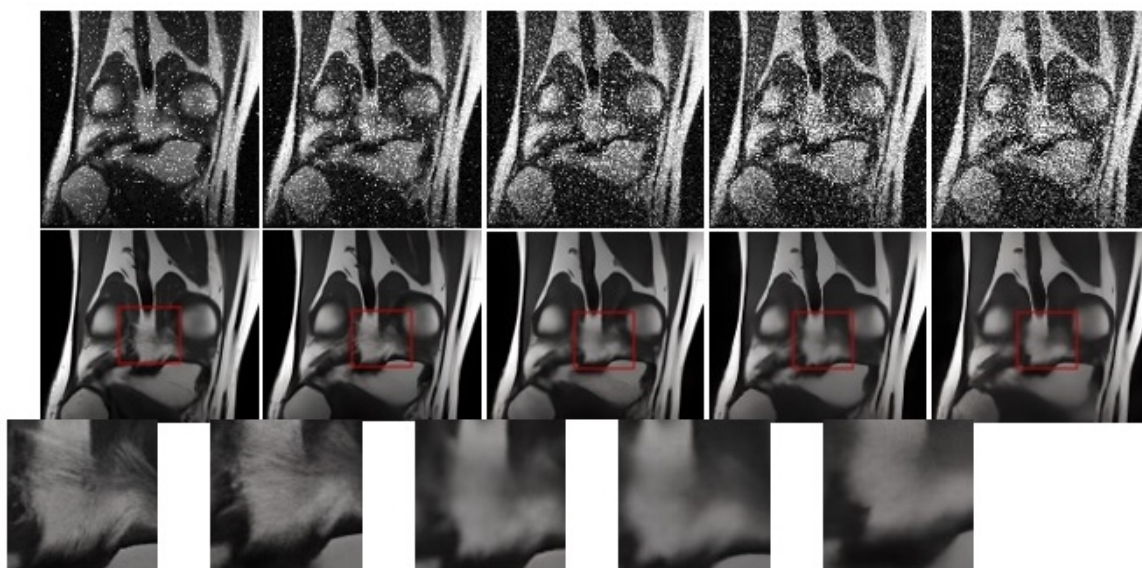


Figure 5: Denoised results for mixed noise with gradually increasing intensity. Our model maintains robust denoising quality despite evolving noise characteristics.

ing prior noise distribution knowledge. Experimental results validate that our method outperforms traditional techniques, particularly in complex, real-world medical imaging scenarios. It achieves high fidelity in noise reduction while preserving essential image details, setting new benchmarks in both quantitative and visual performance.

Future efforts will focus on applying this framework to additional imaging modalities and incorporating cutting-edge neural architectures like generative adversarial networks (GANs) (Goodfellow et al., 2014), potentially redefining the standards for medical image processing. Our results highlight the transformative potential of advanced machine learning in enhancing diagnostic accuracy and expanding clinical applications, laying a robust groundwork for future innovations in medical imaging technology.

## REFERENCES

- Anonymous (2013). Creation of fully sampled mr data repository for compressed sensing of the knee. Proc. SMRT 22nd Annu. Meeting.
- Burger, H. C., Schuler, C. J., and Harmeling, S. (2012). Image denoising: Can plain neural networks compete with bm3d? In *IEEE Conference on Computer Vision and Pattern Recognition (CVPR)*, pages 2392–2399.
- Cherry, S. R., Sorenson, J. A., and Phelps, M. E. (2012). *Physics in nuclear medicine*. Elsevier Health Sciences.
- Dabov, K., Foi, A., Katkovnik, V., and Egiazarian, K. (2007). Image denoising by sparse 3-d transform-domain collaborative filtering. *IEEE Transactions on Image Processing*, 16(8):2080–2095.
- Goodfellow, I. J., Pouget-Abadie, J., Mirza, M., Xu, B., Warde-Farley, D., Ozair, S., Courville, A., and Bengio, Y. (2014). Generative adversarial networks. *arXiv*.
- Ho, J., Jain, A., and Abbeel, P. (2020). Denoising diffusion probabilistic models.
- Jalata, I. K., Khan, R., and Nakarmi, U. (2024). Learning from oversampling: A systematic exploitation of oversampling to address data scarcity issues in deep learning-based magnetic resonance image reconstruction. *IEEE Access*, 12:97621–97629.
- Kim, H., Yie, S. Y., Chun, S. Y., and Lee, J. S. (2022). Purecomb: Poisson unbiased risk estimator based ensemble of self-supervised deep denoisers for clinical bone scan image. In *IEEE 19th International Symposium on Biomedical Imaging (ISBI)*, pages 1–5, Kolkata, India.
- Kim, K., Soltanayev, S., and Chun, S. Y. (2020). Unsupervised training of denoisers for low-dose ct reconstruction without full-dose ground truth. *IEEE Journal on Selected Topics in Signal Processing*, 14(6):1112–1125.
- Lehtinen, J., Munkberg, J., Hasselgren, J., Laine, S., Karras, T., Aittala, M., and Aila, T. (2018a). Noise2noise: Learning image restoration without clean data.
- Lehtinen, J., Munkberg, J., Hasselgren, J., Laine, S., Karras, T., Aittala, M., and Aila, T. (2018b). Noise2noise: Learning image restoration without clean data. In *Proc. of the 35th Int. Conf. on Machine Learning (ICML)*, pages 2965–2974.
- Luisier, F., Blu, T., and Unser, M. (2011). Image denoising in mixed poisson–gaussian noise. *IEEE Transactions on Image Processing*, 20(3):696–708.
- Manjón, J. V. and Coupe, P. (2019). Mri denoising using deep learning and non-local averaging. *arXiv*.



- Metzler, C. A., Mousavi, A., Heckel, R., and Baraniuk, R. G. (2020). Unsupervised learning with stein's unbiased risk estimator. *arXiv preprint arXiv:1805.10531*.
- Ramani, S., Blu, T., and Unser, M. (2008). Monte-carlo sure: A black-box optimization of regularization parameters for general denoising algorithms. *IEEE Transactions on Image Processing*, 17(9):1540–1554.
- Ulyanov, D., Vedaldi, A., and Lempitsky, V. (2018). Deep image prior. In *IEEE Conference on Computer Vision and Pattern Recognition*, pages 9446–9454.
- Ulyanov, D., Vedaldi, A., and Lempitsky, V. (2020). Deep image prior. *International Journal of Computer Vision*, 128(7):1867–1888.
- Zhang, K., Zuo, W., Chen, Y., Meng, D., and Zhang, L. (2017a). Beyond a gaussian denoiser: Residual learning of deep cnn for image denoising. *IEEE Transactions on Image Processing*, 26(7):3142–3155.
- Zhang, K., Zuo, W., Chen, Y., Meng, D., and Zhang, L. (2017b). Beyond a gaussian denoiser: Residual learning of deep cnn for image denoising. *IEEE Transactions on Image Processing*, 26(7):3142–3155.
- Zhussip, M., Soltanayev, S., and Chun, S. Y. (2019). Extending stein's unbiased risk estimator to train deep denoisers with correlated pairs of noisy images. In *Proceedings of the 33rd Conference on Neural Information Processing Systems (NeurIPS)*, Vancouver, Canada.

